



FLEXURAL CAPACITY OF POST-TENSIONED MASONRY WALLS

J. R. Bean¹ and A. E. Schultz²

ABSTRACT

Presently, masonry design codes in some countries, including the United States, contain provisions for the loadbearing use of post-tensioned masonry. These provisions address multiple limit states, including jacking, service condition after losses, and ultimate conditions (i.e., at strength). In order to address the last of these cases, nominal capacity in flexure must be calculated, and previous knowledge on the mechanics of masonry sections in flexure has been adopted for this purpose. This knowledge includes the definition of a compression stress block, and the corresponding formulas for estimating flexural strength. However, other factors must be taken into account in post-tensioned masonry, including the properties of the post-tensioning steel and its location in the masonry cross-section before and after deformation. The latter issue is affected by the manner in which the tendons are placed in the masonry, and, more specifically, whether the tendons are restrained against displacement relative to the masonry cross-section. This paper reviews methods for estimating cross-section flexural strength in post-tensioned masonry walls, as well as the impact of tendon location in unrestrained cross-sections. Test data from several experimental investigations by other researchers are included for comparison in this numerical review.

Key words: clay brick; concrete block; prestressed masonry; post-tensioning; flexure; moment capacity; out-of-plane; restrained tendon; unrestrained tendon.

¹Graduate Research Assistant, Department of Civil Engineering, University of Minnesota, Minneapolis, MN, 55455, USA, bean0032@tc.umn.edu.

²Associate Professor, Department of Civil Engineering, University of Minnesota, Minneapolis, MN, 55455, USA, schul088@tc.umn.edu.

BACKGROUND

Loadbearing masonry, unlike steel and concrete construction, has the capability of incorporating architectural elements, such as partitions and non-loadbearing walls, into structural design without adding significant material or cost to the structure. This feature eradicates the coupled need in modern construction of a load-resisting frame and architectural accessories, thus offering structural advantage and cost effectiveness. However, the structural success of masonry depends on the ability to overcome the intrinsic low tensile strength, either by reinforcing or by prestressing.

Prestressed masonry involves a compressive force applied by the steel placed within the masonry cells, which counteracts tensile stresses resulting from service loads. Two main procedures are used to apply the prestressing force to the steel: pre-tensioning (tendons are tensioned before stress transfer to the masonry) or post-tensioning (tendons are tensioned after the masonry is placed). Between these two methods, post-tensioning is preferred over pre-tensioning because of construction ease and because stress loss from elastic deformation during the prestressing process is avoided.

One technique for post-tensioning, commonly used in the United Kingdom, begins by anchoring a pre-stressing rod to the foundation by anchoring the bottom of the bars into a footing. Brick or block courses are laid around the prestressing rods, and the masonry wall is then capped with bearing pads which allow the prestressing rods to project out the bearing pad. A steel bearing plate is placed on top of the bearing pad, and a nut is threaded onto the protruding rod, which serves as an anchor. After the indicated compressive strength is attained in the masonry, the steel rod is stressed with a torque wrench or hydraulic jack (Schultz and Scolforo, 1991).

Prestressed masonry is a versatile building system, and it features many variables to consider in design, including the level of the prestressing force and the amount of reinforcing. The degree of tendon restraint and the effect of grouting also have a significant impact on the strength of the wall. There are three common conditions for tendon restraint: grouted, guided, and unguided (unrestrained). The grouted condition involves fully grouting the core containing the prestressing tendon after it is stressed. This case is fully restrained since the tendon is not able to freely move within the core. The second condition is guided; where the core is left ungrouted but the prestressing tendon is restrained by inserts adhered to some of the hollow units. This case prevents transverse motion of the rod, but still allows some movement of the tendon since the core is ungrouted. The third condition is unguided where the prestressing tendon is left unrestrained in the core and no grouting is involved. In this case, the rod is able to move freely within the cells of the masonry (Graham and Page, 1995).

Prestressed masonry has been used in a variety of applications: buildings, bridge abutments, storage towers, and in strengthening unreinforced masonry walls. Post-tensioned masonry design assures that structures will remain uncracked while under service loads and that collapse during ultimate loading does not occur.

Code Methods for Analysis of Flexural Strength

In order to ensure safe structures, research in prestressed masonry has been conducted, especially in the last three decades. These studies have shown that masonry under out-of-plane loading generally displays nearly elastic behavior until cracking, ensued by nonlinear behavior until failure. In the case of bonded tendons, post-cracking analysis of the prestressed walls has been founded on strain compatibility between the masonry and steel. For the unbonded case, formulas based on post-tensioned concrete design have sometimes been used (Rodriguez et al., 1998).

In early prestressed masonry design, the stress in the prestressing tendon was defined using Eq. (1), where $\alpha = 0.10$. Schultz and Scolforo (1992) showed that the effective bond factor α implicit in the ACI formulas (ACI, 2000) was less than or equal to 0.1 in most practical cases.

$$\varepsilon_{ps} = \varepsilon_{se} + \alpha \varepsilon_m \quad (1)$$

Phipps (1992) developed an alternate expression, noted as Eq. (2) below, and proposed it for prestressed masonry design practice in Great Britain. This equation has been further adopted by the Masonry Standards Joint Committee (MSJC) and appears in the 1999 MSJC standard.

This paper will review two methods of estimating the cross-section flexural strength in post-tensioned masonry walls: the MSJC method and the American Concrete Institute (ACI) method (ACI 318-99). The MSJC method includes equations for both restrained and unrestrained tendons. The ACI method provides an equation for calculating the nominal moment capacity of post-tensioned concrete sections with restrained tendons only.

In the MSJC provisions, to evaluate the stress for a bonded tendon, the cross section is analyzed assuming strain compatibility between masonry (grout) and tendons. For the unbonded, unrestrained tendon scenario, a moment strength check is not required, so the tendon stress at nominal moment strength is not needed. If the stress is needed, it is conservatively assumed that the effective stress in the tendon equals the stress in the tendon at nominal moment strength ($f_{ps} = f_{se}$). In the unbonded, restrained tendon case, the tendon stress is defined by

$$f_{ps} = f_{se} + \frac{100,000d}{l_p} \left[1 - 1.4 \left(\frac{f_{pu} A_{ps}}{bdf'_m} \right) \right] \quad (2)$$

Further, the compression block depth and moment strength can be calculated using

$$a = \frac{f_{ps}A_{ps} + f_yA_s + P_u}{0.85f'_m b} \quad (3)$$

$$M_n = (f_{ps}A_{ps} + f_yA_s + P_u) \left(d - \frac{a}{2} \right) \quad (4)$$

The ACI provisions (ACI, 2000) for determining tendon stresses in post-tensioned concrete with unbonded, restrained conditions were adopted here without any consideration given to the possible differences between concrete and masonry except for substituting concrete compressive strength f'_c by masonry compression strength f'_m .

For $l_p/d < 35$,

$$f_{ps} = f_{se} + 10,000 + \frac{bdf'_m}{100A_{ps}} \quad (5)$$

and for $l_p/d > 35$,

$$f_{ps} = f_{se} + 10,000 + \frac{bdf'_m}{300A_{ps}} \quad (6)$$

CASE STUDIES

Five research projects, from published technical literature within the last 5 years, provided experimental investigations that were used for comparison in this numerical review. The experimental program for the five studies contained different variables and provided a broad range of data. The data collected from these studies was used to estimate the cross-section flexural strength in post-tensioned masonry walls using both the MSJC and ACI code provisions. The five case studies are described in detail herein.

Case Study 1 – Rodriguez et al. (1998)

The first case is from a study at Drexel University by Rodriguez, Hamid and Larralde (1998). The experimental program consisted of testing four walls, designated W1, W2, W3, and W4, constructed of hollow concrete block with a masonry compressive strength of 27.37 MPa (3970 psi). The dimensions of all four walls were 1.9304 m (76 in) high, 0.6096 m (24 in) wide and 0.1524 m (6 in) thick.

One threaded steel bar was placed in each of the four wall sections. In walls W1 and W4, a 19.1 mm (0.75 in) bar was used for reinforcing, whereas in sections W2 and W3, a 25.4 mm (1 in) bar was utilized. The ultimate tensile strength for the post-tensioning steel was 802.8 MPa (116.5 psi).

The post-tensioning rod was guided by metal restraints were spaced every other course for specimens W1, W2, and W3, and two different schemes were used for these walls. For walls W1 and W3, a small steel plate was used in which a hole was provided for the steel rod to protrude. These plates, embedded in the mortar, were sufficient for wall W1, but for wall W3 the mortar could not resist the lateral force due to the shifting of the prestressing rod, thus causing the plates to push through the mortar. Therefore, a new type of restraint was devised for specimen W2 with two pins welded to the steel plate to offer an interlocking connection with the masonry units. For specimen W4 section, the tendons were unguided.

The initial levels of prestressing for specimens W1 and W2 were 81.3 kN (18,280 lb) and 81.53 kN (18,330 lb), respectively. For wall sections W3 and W4, the initial levels of post-tensioning were 84.56 kN (19,010 lb) and 81.27 kN (18,270 lb), respectively. The prestressing force was monitored during the tests using electronic gauges.

The wall sections were tested in a horizontal position by applying two concentrated line loads at the third points. Simply supported end conditions were simulated by using a roller and pinned end connection.

Case Study 2 – Mojsilovic and Marti (1996)

The second case is from a study by Mojsilovic and Marti (1996) at the Swiss Federal Institute (ETH) in Zurich. This experiment study consisted of six bending tests of cored calcium silicate brick (walls K7 and K8) or hollow clay brick (walls B11-B14) post-tensioned wall specimens. The masonry had a compressive strength of 12.1 MPa (1755 psi) for walls K7, K8 and 10.7 MPa (1552 psi) for walls B11 through B14. The height of the walls was 5.0 m (197 in) for K7, K8, B13, and B14 and 2.6 m (102 in) for walls B11 and B12. The width of all walls was 1.03 m (40.6 in) and the thickness 0.18 m (7.09 in).

Monostrand tendons with an ultimate tensile strength of 1765 MPa (256 ksi) were greased and placed in metal ducts within the cavities of the walls. The cavities were assumed grouted and the tendons restrained. Two 16 mm (0.63 in) strands were used for each wall specimen.

An external concentric compression force was applied to each wall section. Each strand was prestressed to 100 kN (22.5 k). An axial load was also applied to each wall segment: 120 kN (26.98 k) on walls K7, B12, B13 and 360 kN (80.9 k) on walls K8, B11, and B14.

Case Study 3 – Graham and Page (1995).

The third case is an experimental study at the University of Newcastle in Newcastle, Australia by Graham and Page. This experimental program consisted of 26 hollow clay brick wall specimens laid in running bond, with a masonry compressive strength of 15.6 MPa (2262.8 psi). The wall panels were 1.7 m (66.9 in) in height and 0.8 m (31.5 in) wide.

The wall specimens contained one prestressing rod, which was located in the central core of the wall section. Each wall panel contained one of two bar types: a 16 mm (0.30 in) deformed bar (400 MPa nominal yield strength) or a 20 mm (0.787 in) “Threadlock” bar (500 MPa nominal yield strength). The “Threadlock” bar is deformed in such a way that it may also double as a thread, so that it may be connected or secured using the proper coupler. The smaller bars were used to post-tension walls 1F, 2F, 5F, 6F, 10F, 11F, 1S, 2S, 5S, and 8S. The rest of the walls (3F, 4F, 7F, 8F, 9F, 12F, 13F, 14F, 15F, 3S, 4S, 6S, 7S, 9S, 10S, and 11S) were post-tensioned with the larger bars.

The level of the restraint in the wall section was also varied. The restraint conditions, for this case study, varied between the three cases: guided (G), unguided (UG), and grouted (GR). Eight sections were grouted (1F, 2F, 3F, 4F, 1S, 2S, 3S, 4S). Nine of the sections were guided (5F, 6F, 7F, 8F, 9F, 15F, 5S, 6S, 7S) and nine sections were unguided (10F, 11F, 12F, 13F, 14F, 8S, 9S, 10S, 11S).

The effective prestress level also varied between zero, 1 MPa (145 psi), and 2 MPa (290 psi). The wall sections with no effective prestress were 1F, 3F, 5F, 7F, 10F, 12F, 1S, and 3S. The walls with an effective prestress of 1 MPa were 2F, 4F, 6F, 8F, 11F, 13F, 15F, 2S, 4S, 5S, 6S, 8S, and 9S. The remaining four tests were prestressed to 2 MPa. One test (11S) had premature failure from sudden impact loading due to a failure in the loading system, so it did not have an effective prestress level recorded.

Two types of flexural tests were utilized: a four point bending test (to create a constant moment region in the center of the span) and a three point bending test (to cause shear by placing the load on one end of wall section).

Case Study 4 – Lacika and Drysdale (1995)

The fourth case study comes from an experimental investigation at McMaster University in Hamilton, Ontario (Canada) by Lacika and Drysdale (1995). This study contained six walls (w1, w3, and w5-w8) that were constructed of clay brick and which had a compressive strength of 32.0 MPa (4641.7 psi). The walls all were 1.2 m (47.2 in) wide and 0.09 m (3.54 in) thick. The height of the walls was 2.7 m (106.3 in) for specimens w1 and w3, 4.2 m (165.4 in) for specimens w5 and w6, and 6.0 m (236.2 in) for specimens w7 and w8.

The sections were reinforced with one prestressing strand that was 26 mm (1.02 in) in diameter. The prestressing steel minimum ultimate strength was 1030 MPa (149.4 ksi). The deformed prestressing bar was restrained at the center of each of the wall segments.

The wall specimens were simply supported and axial and lateral loading was applied to each. Initially, each wall was prestressed to 57 kN (12.8 k) and then loaded axially up to 500 kN (112.4 k). Then, the walls were unloaded and prestressed to 114 kN (25.6 k) and loaded axially again to 500 kN. The wall was again unloaded, re-prestressed to 170 kN (38.2 k), and loaded axially. After each of these axial loading/prestressing cycles, the walls were loaded transversely and test results recorded. Only the data from the lateral load test following the first axial loading/prestressing cycle for each wall was

included in this study, as the other two transverse load tests represent reloading of partially damaged (cracked) walls.

Case Study 5 – Krause et al. (1996)

The fifth case study is from an experimental investigation at the University of Nebraska in Omaha by Krause, Devalapura, and Tadros. This testing program consisted of a series of bending tests for six wall specimens (TPIUG1, TPIUG2, TPIUG3, TPIG1, TPIG2, TPIG3) made of cored clay brick. The compressive masonry strength was 19.6 MPa (2845 psi) and the walls were 0.914 m (36 in) wide and 0.92 m (3.625 in) thick, and 1.83 m (72 in) tall.

One intermediate grade threaded bar, 38 mm (1.5 in) diameter, was prestressed in the brick cores. The steel had an ultimate strength of 827.2 MPa (120 ksi). Three of the walls were ungrouted (TPIUG1, TPIUG2, TPIUG3) and unrestrained and the three others were grouted and restrained. However, this case study was not included in the final comparisons with the other four case studies due to the limited amount of information available.

RESULTS

Figure 1 summarizes the accuracy of the MSJC and ACI methods for calculating moment capacity of a post-tensioned masonry wall section. The bar graph plots the average values for the ratio of calculated-to-experiment flexural capacity for each of the first four case studies. The case studies were subdivided into the three restraint categories of grouted, guided, and unguided since the code provisions vary for each fixity case.

In Fig. 1, the horizontal line at calculated-to-experimental moment ratio equal to unity represents the ideal situation where calculated moment equals the experimental capacity. Any values above this horizontal line are unconservative (undesirable), since a value greater than unity signifies a calculated moment that overestimates the experimental value. This situation is undesirable in design and should be avoided.

As can be seen in Figure 1, the ACI method is the more accurate of the two methods. An ACI value was not included for the unguided categories because the ACI method does not have a provision for this fixity case. In comparing the methods, the ACI formulas were consistently closer to the measured moment capacities. However, both methods were not overly accurate, as shown for the three categories in Case #3. In this case, the calculated/experimental ratio was less than 0.5, which shows meager precision in estimating the flexural strength of masonry walls.

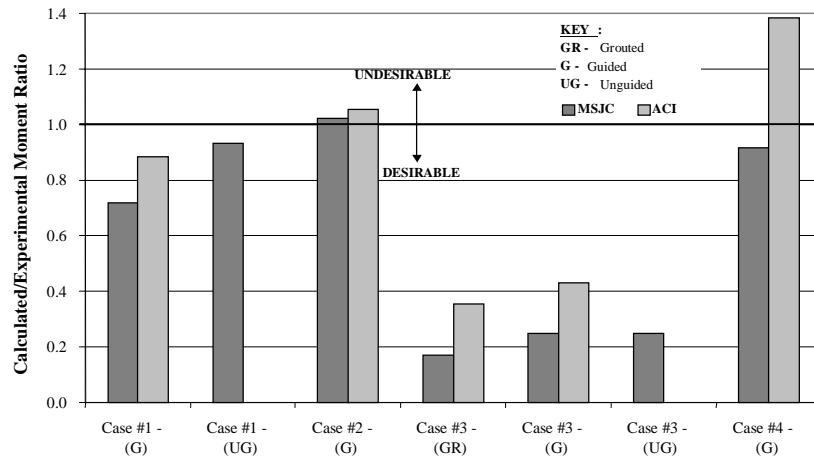


Figure 1. Accuracy of MSJC and ACI Methods

Figure 2 depicts three different methods for calculating the nominal moment capacity. In addition to plotting the ratio of the calculated to experimental flexural strength using the MSJC and ACI methods, the flexural capacity was also calculated using the experimental bar force rather than a calculated one. These calculations were completed for Case Studies 1 and 2 since the experimental force was available in these studies. The calculated/experimental ratio was calculated for each of the different wall specimens in the two case studies.

It can be seen in Fig. 2 that using the experimental bar force resulted in a flexural capacity larger than the experimental value in one-half of the cases. When comparing the data, it was found that the average values of the moment ratios calculated using the experimental bar force, the MSJC procedure, and the ACI method, respectively, were 1.067, 0.921, and 0.998, respectively. However, the standard deviation for the flexural capacity ratio using the experimental bar force was 0.208, which is lower than the standard deviation of 0.262 for the MSJC procedure and 0.242 for the ACI method.

The MSJC method is seen to provide flexural capacity estimates close to (but less than) the measured capacity, but it also features the highest deviation. Flexural capacity ratios obtained using experimental bar forces had the highest average, yet they also had the lowest deviation. The ACI procedure represents the best compromise between precision and accuracy, with an average moment ratio and corresponding standard deviation that are between the corresponding values for other two methods. However, all three methods can stand improvement in terms of their ability to predict flexural capacity, including better estimates of post-tensioning tendon stress at ultimate as well as a more accurate representation of the magnitude and distribution of masonry stresses.

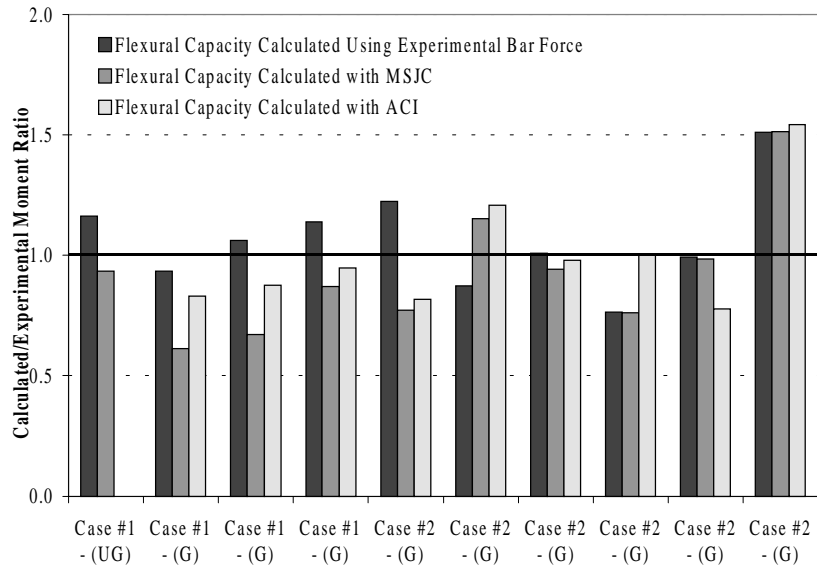


Figure 2. Comparison of Methods

Figure 3 shows calculated-to-experimental moment ratios for the walls plotted according to height-to-thickness (h/t) ratio. While there is some scatter in this data, there also appears to be a clear trend. As slenderness (h/t) increases, so does the tendency of the analysis methods to overestimate moment capacity. In fact, for slenderness ratio h/t equal to 4.0 or larger, all moment ratios are unconservative ($M_{calc}/M_{exp} > 1$). There appears to be a decrease in moment capacity with increasing slenderness ratio that the three analysis methods cannot reproduce.

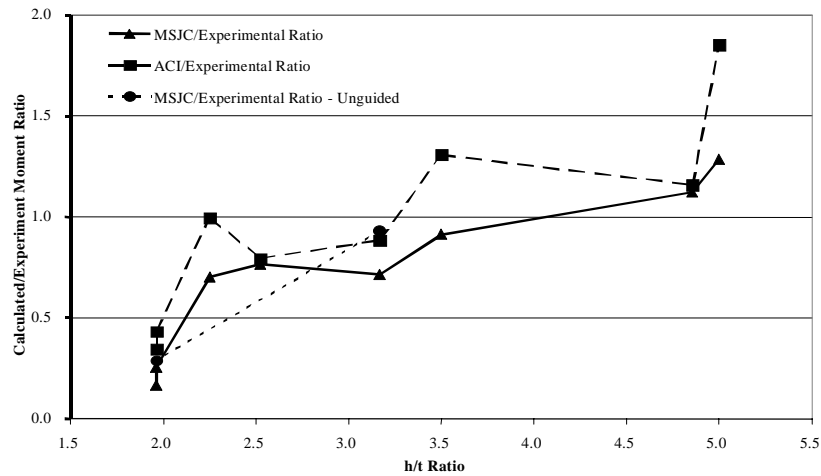


Figure 3. Influence of Slenderness (h/t) Ratio on Flexural Strength

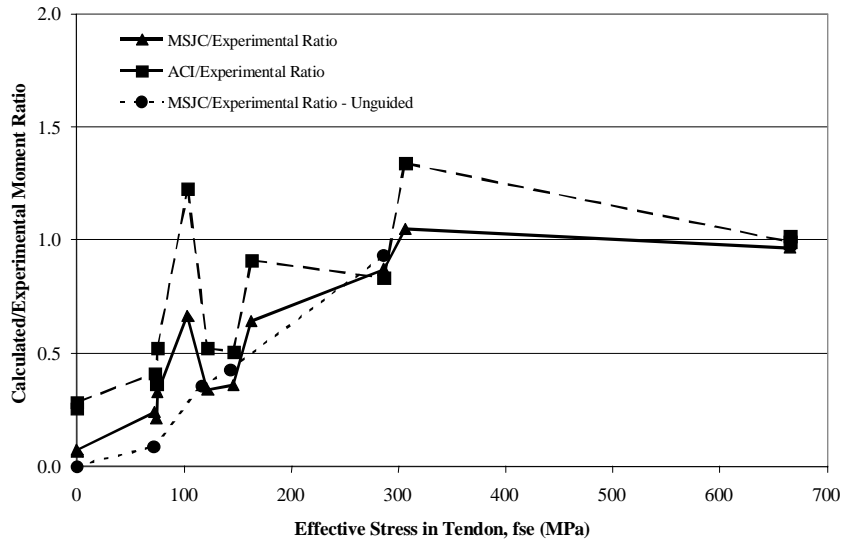


Figure 4. Influence of Tendon Effective Stress on Flexural Strength

Figure 4 illustrates the influence of effective stress in the tendon on the ability of the three methods to predict flexural strength. The vertical axis indicates the calculated-to-experiment moment ratio, and the horizontal axis shows the effective stress in the tendon (f_{se}) after losses, but before any transverse loading. Once again, there is some scatter in the data, but it can be seen that as effective stress increases, there is a general increase in the amount by which the ACI and MSJC methods overestimate flexural capacity. This observation suggests that as f_{se} increases, the methods cannot predict the change (decrease) in cross-section resistance. It is further noted that for $f_{se} > 300$ MPa, the calculated-to-predicted moment ratios are equal to or exceed unity.

Another interesting aspect of the data, but which is not apparent in Fig. 4, is that finite (non-zero) moment capacities were recorded by wall specimens that featured unguided tendons, and which had initial prestress magnitudes equal to zero. It is generally assumed in design that there is little or no change in the tendon stress magnitude of unguided tendons due to bending from transverse loading. Consequently, the ACI and MSJC procedures assign a calculated moment capacity equal to zero for such walls, assuming no external axial load either. Yet, these specimens developed non-zero moment capacities. That can only occur if, contrary to the common opinion, bending generates stress increases in unguided tendons.

Figure 5 is similar to Fig. 4 except that the tendon stresses shown are at nominal flexural capacity. The trend is very similar to that observed in Fig. 4 for tendon effective stress. The only significant difference is that most of the calculated-to-experimental moment ratios are less than or equal to unity. This fact is reassuring in that resulting designs are conservative, i.e. moment capacities were not overestimated. However, this observation also indicates that calculated design capacities for tendon stresses $f_{ps} < 200$ MPa are very over conservative, with calculated flexural strengths less than 50% of the

measured experimental moments.

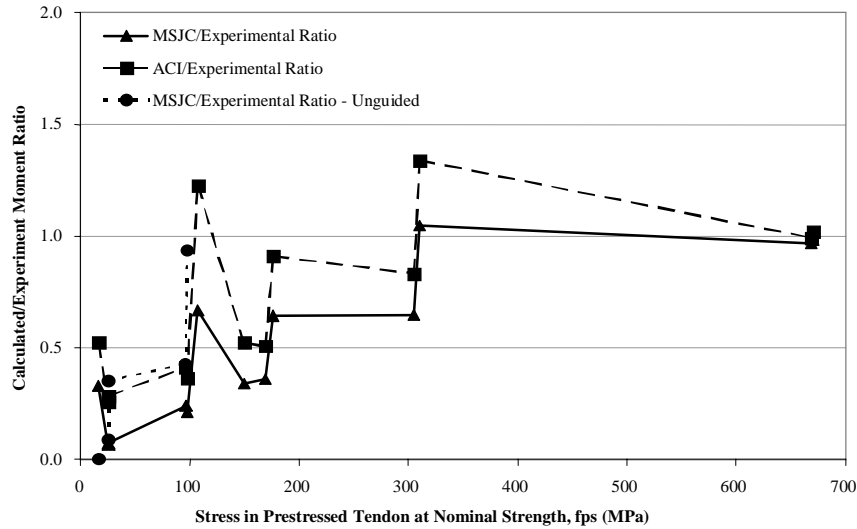


Figure 5. Influence of Tendon Stress at Nominal Strength

CONCLUSIONS

Through the analysis of five case studies, a need for reevaluating of U.S. code procedures for calculating the out-of-plane flexural capacity of post-tensioned walls has been demonstrated. The ACI and MSJC methods showed a dependency in the accuracy of calculated moment capacity with slenderness ratio (h/t), tendon effective stress (f_{se}), and tendon stress at nominal capacity (f_{ps}). As slenderness ratio, or tendon stress, increases, the tendency for the ACI and MSJC analysis procedures to overestimate flexural capacity increase. The problem appears to be not only with the estimation of tendon stresses at ultimate, but also with the characterization of cross-section resistance. An unexpected finding of this numerical review is the moment capacity increase experienced by wall specimens with unguided tendons that have little or no initial prestress ($f_{se} \approx 0$). It suggests that current design methods in the US do not represent accurately the stress increase with bending in walls with unguided tendons. A more dependable and consistent method of analysis needs to be developed for such walls.

ACKNOWLEDGEMENTS

This research was conducted with financial support from the National Science Foundation through grant CMS-9904110, V. J. Gopu, Program Director, and the Graduate School of the University of Minnesota, Twin Cities by means of a Fellowship to the first author. This support is gratefully acknowledged.

REFERENCES

- ACI 318-95, (1998). *Building Code Requirements for Reinforced Concrete*. American Concrete Institute, September, pp. 260.
- Graham, K.J. and Page, A.W., (1995). "The Flexural Design of Post-Tensioned Hollow Clay Masonry." Proceedings of the 7th Canadian Masonry Symposium, Hamilton, Ontario, June, pp 763-774.
- Krause, G.L, Devalapura, R. and Tadros, M.K, (1996). *Worldwide Advances of Structural Concrete and Masonry*. Proceedings of the CCMS Symposium, ASCE, Chicago, Illinois, April, pp.37-48.
- Lacika, Edward M. and Drysdale, Robert G., (1995). "Experimental Investigation of Slender Prestressed Brick Walls." Proceedings of the 7th Canadian Masonry Symposium, Hamilton, Ontario, June, pp 724-735.
- Masonry Standards Joint Committee, (1999). *Building Code Requirements for Masonry Structures*. TMS, ACI, and ASCE, pp. C-26.
- Mojsilovic, N. and Marti, Peter, (1996). "Load Tests on Post-Tensioned Masonry Walls." Proceedings of the 7th North American Masonry Conference, South Bend, Indiana, USA, June, pp. 327-335.
- Phipps, M.E., (1992). "The Codification of Prestressed Masonry Design." Proceedings of the 6th Canadian Masonry Symposium, Saskatoon, Saskatchewan, Canada, June, pp. 561-571.
- Rodriguez, R., Hamid, A. A., and Larralde, J., (1998). "Flexural Behavior of Post-Tensioned Concrete Masonry Walls Subjected to Out-of-Plane Loads." *ACI Structural Journal*, Vol. 95, No. 1, January-February 1998, pp. 61-70.
- Schultz, A.E. and Scolforo, M. J., (1991). "An Overview of Prestressed Masonry." *The Masonry Society Journal*, Vol. 10, No. 1, August, pp 6-21.
- Schultz, A.E. and Scolforo, M. J., (1992). "Engineering Design Provisions for Prestressed Masonry." *The Masonry Society Journal*, Vol. 10, No. 2, pp. 29-64.

NOTATION

- a Depth of rectangular stress block
- A_{ps} Area of prestressing steel
- A_s Area of reinforcing steel
- b Section width
- d Distance from extreme compression fiber to centroid of tension reinforcing
- f'_m Masonry compression strength
- f_{ps} Tensile stress in tendon at nominal strength
- f_{pu} Specified tensile strength of tendon
- f_{se} Effective prestressing stress after all losses
- f_y Specified yield strength of steel
- h Member height
- l_p Clear span of member
- M_n Nominal moment capacity
- P_u Factored Axial Load
- ϵ_m Vertical compression strain in masonry
- ϵ_{ps} Vertical compression strain in prestressing steel (ϵ_{se} after all losses)

Conversion Factors: 1 inch = 0.0254 m; 1 psi = 6.894 Pa; 1 lb = 4.448 kN